

RESEARCH

Open Access



High isolation MIMO antenna for 5G C-band application by using combination of dielectric resonator, electromagnetic bandgap, and defected ground structure

Efri Sandi^{*} , Aodah Diamah and Mumtaz Al Mawaddah

^{*}Correspondence:
efri.sandi@unj.ac.id

Department of Electronics
Engineering, Faculty
of Engineering, Universitas
Negeri Jakarta, Rawamangun,
Jakarta Timur 13220, Indonesia

Abstract

High isolation between massive MIMO antenna elements is one of the important parameters that improves antenna performance, especially for 5G communication applications. In this study, we propose a design to improve isolation between elements to enhance the antenna performance. The proposed solution to improve the performance of massive MIMO antennas is to use a combination of dielectric resonator, electromagnetic bandgap (EBG) and defected ground structure (DGS) techniques at the frequency band 3.5 GHz as the 5G frequency band under 6 GHz. The material used is FR-4 which has a dielectric constant (ϵ_r) of 4.3. Simulation results and measurements between antenna elements show an improvement in mutual coupling, widening the bandwidth and increasing the gain of the antenna. The proposed design using the dielectric resonator antenna (DRA) by MIMO 8×8 16 port—64 elements and the addition of EBG and DGS structures on the ground plane—has shown to suppress mutual coupling parameter lower than without using DRA-EBG-DGS design by 15 dB, increase bandwidth to 246 MHz, increase gain to 24.7 dB and improve the overall envelope correlation coefficient (ECC) parameter.

Keywords: Antenna isolation, Dielectric resonator, Electromagnetic bandgap, Defected ground structure, ECC

1 Introduction

The development of cellular communication technology has entered the fifth generation (5G) which has specifications for high data rates (throughput), low latency, high connection users per square-km, high-capacity mobility, and low power consumption [1]. One of the key technologies that support the high-speed 5G network is the support from antenna capabilities that have multiple-input multiple-output (MIMO) specifications, large number of elements, beamforming capabilities, and wide bandwidth [2, 3].

MIMO capability supports 5G network performance because it can increase signal transmission paths which will improve signal-to-noise ratio (SNR) [4]. Thus, the MIMO

antenna design is one of the basic requirements in the development of 5G antenna technology [5].

In the development of MIMO antennas for 5G applications, microstrip antennas are the most widely chosen because of their low profile, easy placement, and compact size. However, microstrip antennas are inseparable from various limitations, such as narrow bandwidth and low gain [6], especially for the development of MIMO antennas that have massive elements, the emergence of a high mutual coupling effect between adjacent elements [7]. The mutual coupling effect causes a decrease in the quality of the antenna parameters due to electromagnetic interference from two or more antennas that are too close together. The mutual coupling effect is kept to a minimum because it affects the performance of each MIMO antenna. This has become one of the main focuses and issues in the development of MIMO antennas, especially microstrip antennas which have a surface wave effect on the substrate.

The results of studies related to the development of massive MIMO antennas have been submitted previously in a few studies and antenna designs, but further studies are still needed to find better performance solutions and meet 5G technology specifications [7, 8]. A few techniques and analysis of 5G MIMO antenna design have been proposed previously, such as tapered-slot technique [9], dual-slant method [10], substrate integrated waveguide (SIW) technique [11], printed array clutched application [12], and studies about the defected ground structure (DGS) [13]. The results of this study have shown that the performance of the MIMO antenna is sufficient to meet the standard, but not yet in the application of a larger number of elements. Massive MIMO antenna design with many elements will certainly cause radiation interference between elements. For this reason, a solution is needed to increase the isolation between elements [14, 15]. Several studies to improve the isolation of massive MIMO antennas have been proposed previously, such as the development of a dielectric resonator antenna (DRA) [16–21], using a frequency selective surface wall [22, 23], using parasitic elements [24], using an antenna filtering method [25], and adding stacked patch antenna design [7]. Besides, it is also proposed a combination of dielectric resonator design with shielded metasurface [26], fractal design techniques to increase radiation efficiency [27–30], and decoupling technique to improve isolation between elements to improve antenna performance [31–35].

The results of these studies show that performance is in accordance with the standard, but still needs to be improved to achieve better performance, such as lower ECC parameters for many elements and higher gain. Thus, the 5G MIMO antenna that is designed can support greater data transmission capabilities. For this reason, this study will be further investigated through a combination of several existing techniques such as decoupling and dielectric resonator techniques by adding electromagnetic bandgap (EBG) and DGS approaches. This effort is expected to be able to further suppress the mutual coupling effect between MIMO antenna elements, which has an impact on lower ECC parameter performance and significantly increased antenna gain.

The presentation of this paper consists of the background and problems in the first section, then an explanation of the research method in the second section, continued with the proposed design in the third section, the results and discussion in the fourth section, and conclusions and recommendations in the fifth section as a closing.

2 Method and experiment

The flow of the implementation of this study begins with studying the design methods of DRA, EBG, and DGS on the development of massive MIMO antennas. Furthermore, the CST microwave studio software simulation was carried out to obtain the results and performance of the combination of the three methods of changing the structure of the microstrip antenna. The simulation is continued repeatedly with various optimizations if the results have not reached the desired performance. After obtaining improved results, fabrication and measurements are carried out to ensure the results meet the expected performance. This flow is as shown in Fig. 1.

3 Proposed design

To determine the effect of the use of DRA-EBG-DGS on the performance of the massive MIMO antenna, this study was conducted by comparing several parameters of the massive MIMO antenna without the use of DRA-EBG-DGS with the performance of the use of DRA-EBG-DGS on the 8×8 massive MIMO antenna.

3.1 8×8 MIMO design without DRA-EBG-DGS

MIMO antenna design begins with a single patch antenna following the general equation in designing a microstrip antenna using a transmission line approach [36] with an equation approach:

$$W_p = \frac{c}{2f_r \sqrt{\frac{\epsilon_r + 1}{2}}} \quad (1)$$

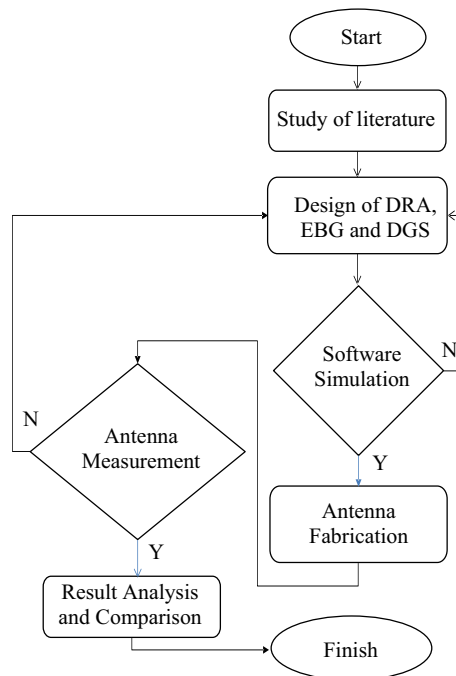


Fig. 1 Design method of massive MIMO DRA-EBG-DGS

$$\varepsilon_{\text{eff}} = \frac{\varepsilon_r + 1}{2} + \frac{\varepsilon_r - 1}{2} \left(\frac{1}{\sqrt{1 + 12 \frac{h}{W_p}}} \right) \quad (2)$$

$$L_{\text{eff}} = \frac{c}{2f_r \sqrt{\varepsilon_{\text{eff}}}} \quad (3)$$

$$\Delta L = 0.412h \frac{(\varepsilon_{\text{eff}} + 0.3) \left(\frac{W_p}{h} + 0.264 \right)}{(\varepsilon_{\text{eff}} - 0.258) \left(\frac{W_p}{h} + 0.8 \right)} \quad (4)$$

$$L_p = L_{\text{eff}} - 2\Delta L \quad (5)$$

$$W_g = 6h + W_p \quad (6)$$

$$L_g = 6h + L_p \quad (7)$$

L_p is the length of patch antenna element, W_p is the width of patch antenna element, and h is the height of patch antenna element. W_g is the width of the ground plane, ε_r is the permittivity relative, and L_g is the length of the ground plane. In this study, the substrate material is Epoxy FR-4 with $\varepsilon_r = 4.3$ and the antenna frequency is 3.5 GHz as one of the 5G C-band frequency bands under 6 GHz. Dimensions of the design results are shown in Table 1.

Then proceed with designing an 8×8 array configuration with 8 elements in the x -axis direction and 8 elements in the y -axis direction with a distance between elements $\lambda/2$. The design results are as in Fig. 2.

3.2 8×8 MIMO design using DRA-EBG-DGS

The proposed design using this DRA-EBG-DGS combination is to place a dielectric resonator on the patch antenna and add an EBG structure between the MIMO antenna elements. Then do the arrangement of the DGS structure on the ground plane structure. The design stage using a dielectric resonator begins with the calculation of the diameter and height. The dimensional design approach follows equation [37]:

$$F_r = \frac{c}{2\pi r \sqrt{\varepsilon_{\text{DRA}}}} \left[1.71t \frac{r}{h} + 0,1578 \left(\frac{r^2}{h} \right) \right] \quad (8)$$

Table 1 Dimension of patch antenna

No	Dimension	Size (mm)
1	W_p	26.32
2	L_p	20.46
3	W_g	35.92
4	L_g	30.06

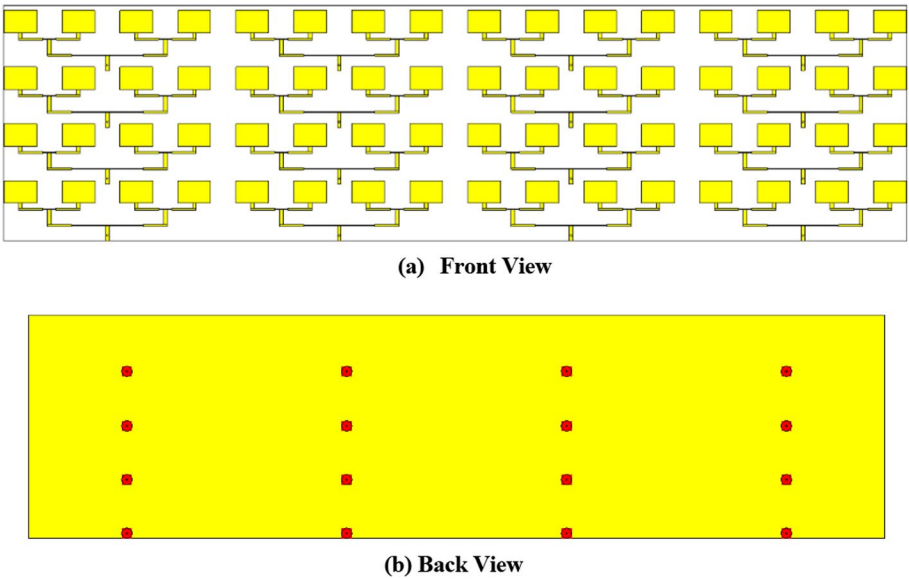


Fig. 2 Design of 8 × 8 massive MIMO antenna without DRA-EBG-DGS

where c is the speed of light, r is radius, h is the height, t is the width of the microstrip, and ϵ_{DRA} is coefficient which value 9.9% for alumina ceramic material. The calculation and design results are shown in Table 2 and Fig. 3.

Furthermore, for the EBG design approach using the mushroom form using the following equation approach [38]:

$$L = \mu_0 h \tag{9}$$

Table 2 Dimension of DRA

No	Parameter	Size (mm)
1	r	27.00
2	h	37.50
3	t	3.137
4	L	66.80

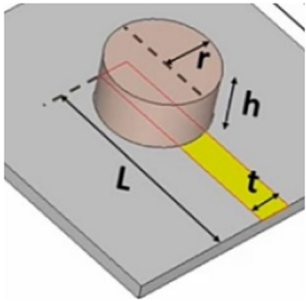


Fig. 3 Design of DRA

Table 3 Dimension of EBG

Dia. Via	Length	Width	Spacing
3 mm	4 mm	4 mm	7 mm

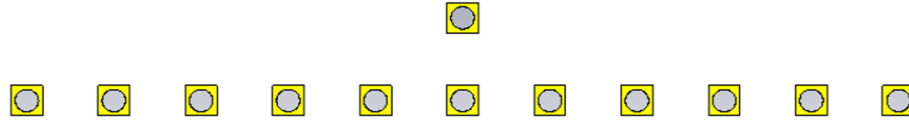
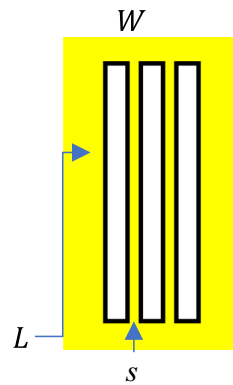

Fig. 4 Design of EBG

Table 4 Dimension of DGS

Length (L)	Width (W)	Spacing (s)
50 mm	4 mm	2 mm


Fig. 5 Design of DGS

$$C = \frac{W \varepsilon_0 (1 + \varepsilon_0)}{\pi} \cosh \frac{(2W + g)}{g} \quad (10)$$

h is the substrate thickness, μ_0 is the permeability of free space, W is the EBG patch width, ε_0 is the permittivity of free space, and g is the gap between two EBG cell. The results of the design and optimization are shown in Table 3 and Fig. 4.

Furthermore, DGS is designed using a microstrip line approach [39] by optimizing the length, width, and distance between the microstrip lines. The results of the DGS design are shown in Table 4 and Fig. 5.

Thus, the use of DRA-EBG-DGS can be developed in the 8×8 massive MIMO antenna configuration as shown in Fig. 6.

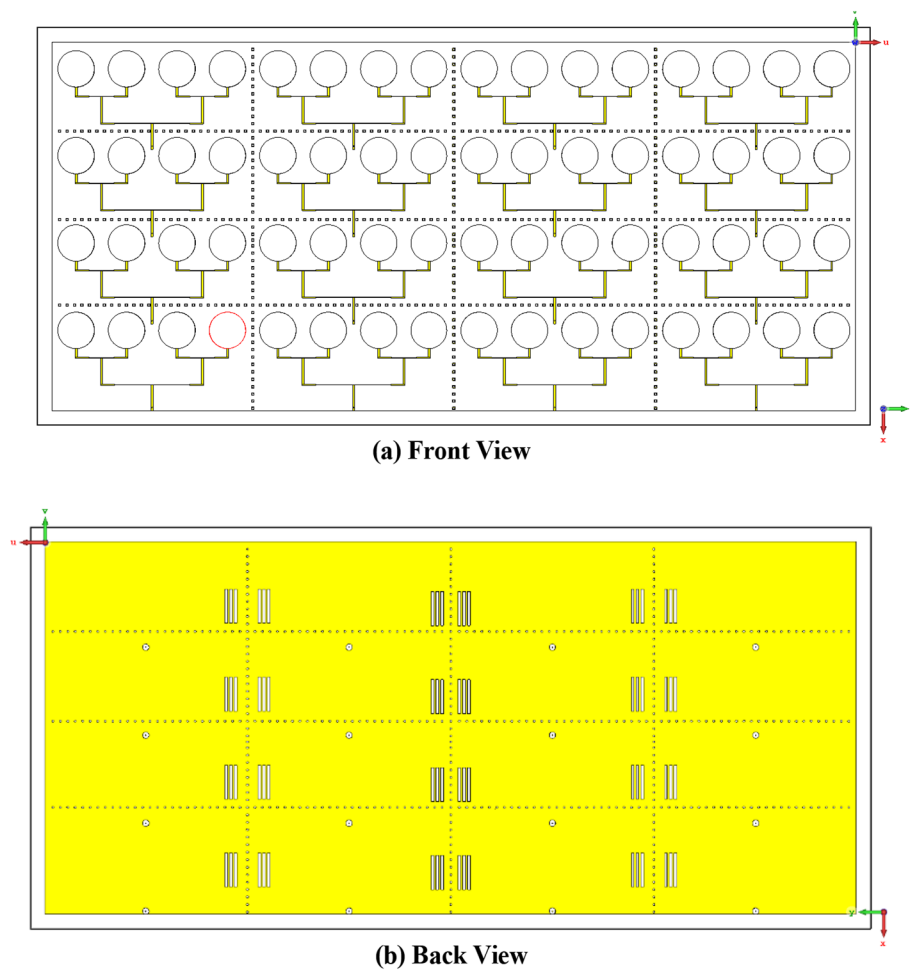


Fig. 6 Design of 8×8 massive MIMO antenna using DRA-EBG-DGS

4 Result and discussion

The simulation results in this study use CST Microwave Studio simulation software to obtain results and comparisons of massive MIMO antennas using DRA-EBG-DGS with conventional massive MIMO antennas without using DRA-EBG-DGS. The comparison of S-parameters can be seen in Fig. 7.

These results indicate that the effect of using DRA-EBG-DGS can widen the bandwidth of the massive MIMO 8×8 antenna to 246 MHz. This result is quite significant without using DRA-EBG-DGS which only has a bandwidth of 145.4 MHz.

The next simulation is a two-dimensional (2D) radiation pattern. The simulation results of this radiation pattern are shown in Fig. 8. We used the beam direction from -60° to 60° . These results indicate that the massive MIMO design using DRA-EBG-DGS can increase the gain to 24.7 dB compared to 19.5 dB without using DRA-EBG-DGS. This result is significant and proves that this proposed design can increase the antenna gain to a higher level.

The next simulation result is a comparison of the 360° polar radiation pattern from the CST simulation software. These results confirm the direction of the massive

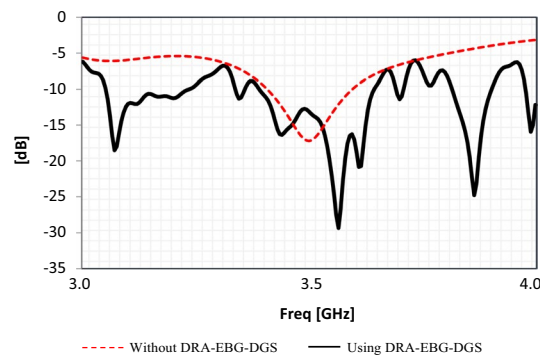


Fig. 7 Simulation result of S-parameter

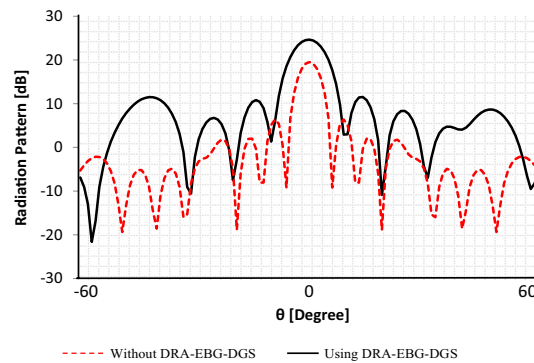


Fig. 8 Simulation result of 2D radiation pattern

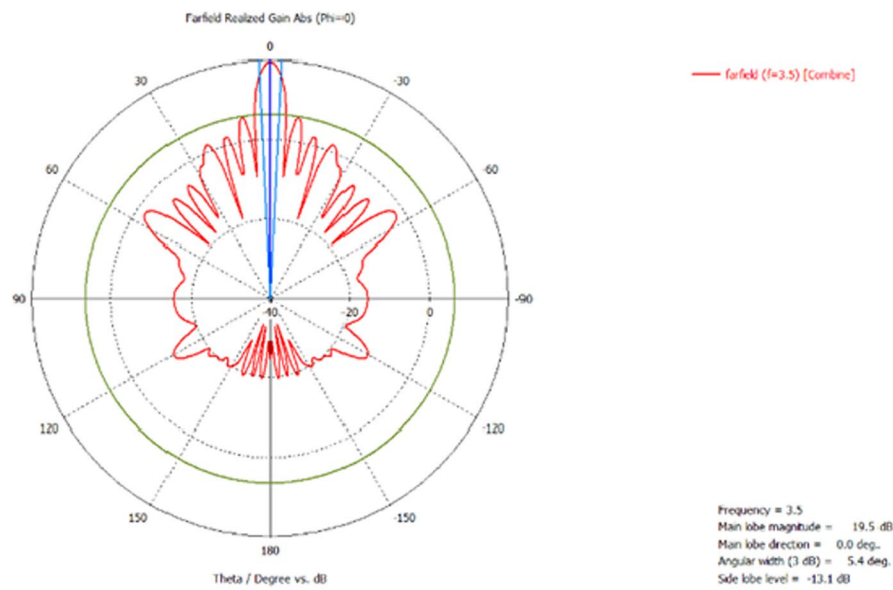
MIMO 8×8 antenna radiation beam in all directions and show the resulting beam-width. The simulation results of the 360° radiation pattern are shown in Fig. 9.

These results show a comparison of the 360° radiation pattern of the massive MIMO 8×8 antenna using DRA-EBG-DGS and without using DRA-EBG-DGS, where there is an increase in the beamwidth of the massive MIMO antenna using DRA-EBG-DGS to be 8.4° wider than without. DRA-EBG-DGS is only 5.4° (Fig. 9).

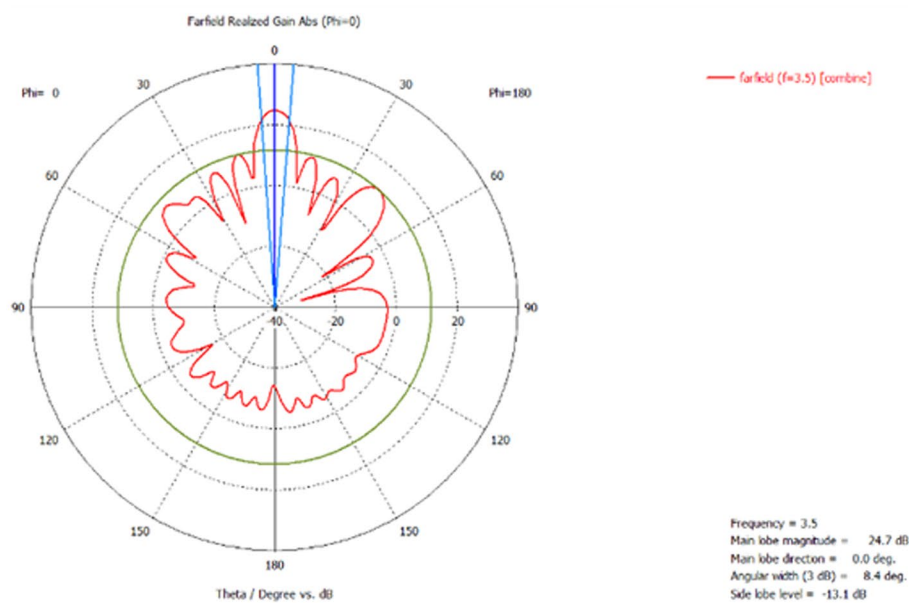
Furthermore, to verify the simulation results, we fabricated a massive MIMO antenna using DRA-EBG-DGS. For the fabrication sample, we only do a comparison using a 4×4 MIMO configuration which is assumed to be representative for a larger number of arrays as show in Fig. 10.

Figure 11 shows the comparison of the S-parameter massive MIMO antenna 4×4 simulation results and measurements. These results show that there is no significant difference between the simulation results and measurements. The difference is only due to the measurement installation factor which has an additional loss so that the measurement results slightly decrease.

Figure 12 shows a comparison of the 2D radiation pattern between the simulation results and measurements of the 4×4 massive MIMO antenna. Similar to the results of the S-parameter comparison, the comparison of simulation results and measurements of 2D radiation patterns also does not show a significant difference, the



(a) Without DRA-EBG-DGS



(b) Using DRA-EBG-DGS

Fig. 9 Simulation result of 360° radiation pattern

difference is only due to not ideal measurement conditions, and there are several loss factors for antenna measurement installations.

As the result in this study, we observe the effect of using DRA-EBG-DGS on the performance of the ECC parameter which is the benchmark for MIMO antenna performance. The simulation results of the comparison of the effect of using DRA-EBG-DGS on ECC parameters are shown in Table 5.

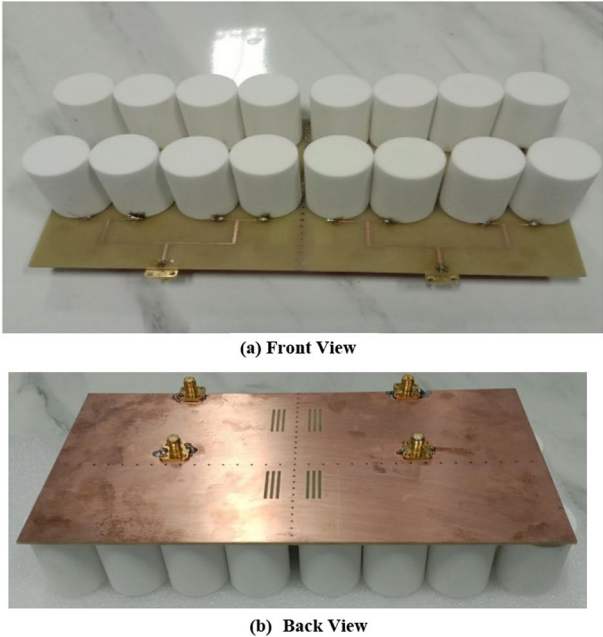


Fig. 10 Fabrication antenna massive MIMO 4 × 4

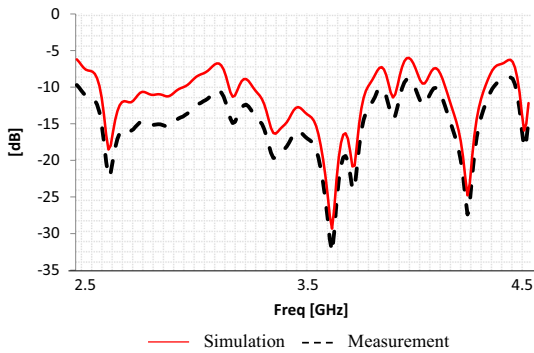


Fig. 11 Comparison of S-parameter 4 × 4 massive MIMO antenna

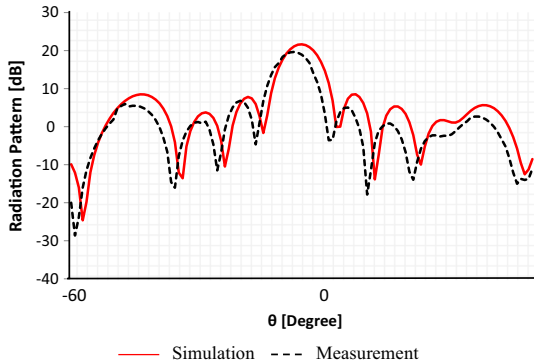


Fig. 12 Comparison of 2D radiation pattern 4 × 4 massive MIMO antenna

Table 5 Comparison of ECC parameter

No	Parameter	Without DRA-EBG-DGS	Using DRA-EBG-DGS
1	ECC 4,1	$1.6576574e^{-006}$	$1.418422e^{-009}$
2	ECC 13,1	$2.5711838e^{-010}$	$6.5478395e^{-0-10}$
3	ECC 3,2	$1.6900828e^{-006}$	$1.1577023e^{-010}$
4	ECC 7,2	$1.9692232e^{-006}$	$9.773286e^{-010}$
5	ECC 5,4	$1.9692972e^{-006}$	$9.6981901e^{-010}$
6	ECC 8,5	$1.6906198e^{-006}$	$1.2061462e^{-010}$
7	ECC 7,6	$1.6582159e^{-006}$	$1.3925197e^{-009}$
8	ECC 10,6	$2.5717832e^{-010}$	$6.5314213e^{-010}$
9	ECC 10,9	$1.8120096e^{-006}$	$5.057252e^{-008}$
10	ECC 13,10	$2.0289825e^{-006}$	$1.9538566e^{-010}$
11	ECC 12,11	$1.8123816e^{-006}$	$5.055012e^{-008}$

Table 5 shows that the use of DRA-EBG-DGS in the massive MIMO antenna design can suppress the mutual coupling effect and improve the ECC parameters. The results show a significant improvement in the ECC parameter so that it can prove that the DRA-EBG-DGS design is effective in the design of the massive MIMO antenna.

5 Conclusions

Massive MIMO antenna design using the DRA-EBG-DGS combination for 5G C-band applications has been described. The simulation and measurement results show a significant improvement in the performance of the massive antenna when using the DRA-EBG-DGS combination. The results of this study show an improvement in the value of the antenna bandwidth and an increase in antenna gain and slightly widen the antenna beamwidth. The most important result is the improvement of the ECC parameter which is an important indicator of the performance of a massive MIMO antenna which has many elements, where a lower ECC parameter will support the overall network performance.

The results of this study are a basic proposal that can be the foundation for the development of a massive MIMO antenna design for 5G applications. In the future, it can be continued by studying further the DRA structure and its effect on the performance of the massive MIMO antenna with various other structural components.

Abbreviations

DRA	Dielectric resonator antenna
5G	5th generation
EBG	Electromagnetic bandgap
DGS	Defected ground structure
MIMO	Multiple input multiple output
ECC	Envelope correlation coefficient
SNR	Signal-to-noise ratio
SIW	Substrate integrated waveguide

Acknowledgements

The datasets analyzed during the current study are not publicly available since they involve a confidentiality agreement but are available from the corresponding author upon reasonable request.

Author contributions

ES conceived the idea. ES completed the MIMO Antenna 5G and wrote this paper. AD and MA contributed to the review of the manuscript. All authors read and approved the final manuscript.

Funding

This work was supported in part by the Ministry of Research, Technology and Higher Education the Republic of Indonesia for research scheme Innovation Research LPPM UNJ under contract number 376/UN39/HK.02/2022.

Availability of data and materials

Data sharing not applicable to this article as no datasets were generated or analyzed during the current study.

Declarations

Competing interests

The authors declare that they have no competing interests.

Received: 7 November 2022 Accepted: 20 December 2022

Published online: 27 December 2022

References

1. D. Warren, and C. Dewar, Understanding 5G: perspectives on future technological advanced in mobil, GSMA Intelligence, 2014.
2. E.L. Bengtsson, F. Rusek, S. Malkowsky, F. Tufvesson, P.C. Karlsson, O. Edfors, A simulation framework for multiple-antenna terminal in 5G massive MIMO systems. *IEEE Access* **5**, 26819–26831 (2017)
3. A.L. Swindlehurst, E. Ayanoglu, P. Heydari, F. Capolino, Millimeter-wave massive MIMO: The next generation revolution? *IEEE Commun. Mag.* **52**, 56–62 (2014)
4. P. Xingdong, H. Wei, Y. Tianyang, L. Linsheng, Design and implementation of an active multibeam antenna system with 64 RF channels and 256 antenna elements for massive MIMO application in 5G wireless communications. *China Commun.* **11**(11), 16–23 (2014)
5. E. Sandi, A. Rusmono, K.V. Diamah, Ultra-wideband microstrip array antenna for 5G millimeter-wave applications. *J. Commun.* **15**(2), 198–204 (2020)
6. R. Garg, *Microstrip antenna design handbook* (Artech House, Boston, 2000)
7. Y. Gao, R. Ma, Y. Wang, Q. Zhang, C. Parini, Stacked patch antenna with dual-polarization and low mutual coupling for massive MIMO. *IEEE Trans. Antennas Propag.* **64**(1), 4544–4549 (2016)
8. T. Tuovinen, N. Tervo, A. Parssinen, Analyzing 5G RF system performance and relation to link budget for directive MIMO. *IEEE Trans. Antennas Propag.* **65**(12), 6636–6645 (2017)
9. B. Yang, Z. Yu, Y. Dong, J. Zhou, W. Hong, Compact tapered slot antenna array for 5G millimeter-wave massive MIMO systems. *IEEE Trans. Antennas Propag.* **65**(12), 6721–6727 (2017)
10. M.V. Komandla, G. Mishra, S.K. Sharma, Investigations on dual slant polarised cavity-backed massive MIMO antenna panel with beamforming. *IEEE Trans. Antennas Propag.* **65**(12), 6794–6799 (2017)
11. E. Sandi, A. Diamah, M.W. Iqbal, D.N. Fajriah, Design of substrate integrated waveguide to improve antenna performances for 5G mobile communication application. *J. Phys.: Conf. Ser.* **1402**(4), 04403 (2019)
12. C. Lee, M.K. Khattak, S. Kahng, Wideband 5G beamforming printed array clutched by LTE-A 4x4-multiple-input-multiple-output antennas with high isolation. *IET Microw. Antennas Propag.* **12**(8), 1407–1413 (2018)
13. K.R. Mahmoud, A.M. Montaser, Optimized 4x4 millimetre-wave antenna array with DGS using hybrid ECFO-NM algorithm for 5G mobile networks. *IET Microw. Antenna Propag.* **1**(11), 1516–1523 (2017)
14. Y. Li, C.D. Sim, Y. Luo, G. Yang, High-isolation 3.5 GHz eight-antenna MIMO array using balanced open-slot antenna element for 5G smartphones. *IEEE Trans. Antennas Propag.* **67**(6), 3820–3830 (2019)
15. W. Jiang, Y. Cui, B. Liu, W. Hu, Y. Xi, A dual-band MIMO antenna with enhanced isolation for 5G smartphone applications. *IEEE Access* **7**, 112554–112563 (2019)
16. Y. Zhang, J. Deng, M. Li, D. Sun, L. Guo, A MIMO dielectric resonator antenna with improved isolation for 5G mm-wave applications. *IEEE Antennas Wirel. Propag. Lett.* **18**(4), 747–751 (2019)
17. J. Tan, J.T. Bernhard, Design of a MIMO dielectric resonator antenna for LTE femtocell Base Station. *IEEE Trans. Antennas Propag.* **60**(2), 438–444 (2012)
18. A. Abdalrazik, A.S.A. El-Hameed, A.B. Abdel-Rahman, A Three-port MIMO dielectric resonator antenna using decoupled modes. *IEEE Antennas Wirel. Propag. Lett.* **16**, 3104–3107 (2017)
19. M.S. Sharawi, S.K. Podilchak, M.U. Khan, Y.M. Antar, Dual-frequency DRA-based MIMO antenna system for wireless access points. *IET Microw. Antenna Propag.* **11**(8), 1174–1182 (2017)
20. H.I. Kremer, K.W. Leung, M.W.K. Lee, Design of substrate-integrated dielectric resonator antenna with dielectric vias. *Trans. Antennas Propag.* **69**(9), 5205–5214 (2021)
21. M. Boyuan, J. Pan, Comments on "A semi-analytical model of high-permittivity dielectric ring resonators for magnetic resonance imaging." *Trans. Antennas Propag.* **70**(4), 3128–3130 (2022)
22. Hu. Yafei, Decoupling and low-profile design of dual-band dual-polarized base station antennas using frequency-selective surface. *IEEE Trans. Antennas Propag.* **67**(8), 5272–5281 (2019)
23. R. Karimian, A. Kesavan, M. Nedil, T.A. Denidni, Low-Mutual coupling 60 GHz MIMO antenna system with frequency selective surface wall. *IEEE Antennas Wirel. Propag. Lett.* **16**, 373–376 (2017)
24. Z. Li, Z. Du, M. Takahashi, K. Saito, K. Ito, Reducing mutual coupling of MIMO antennas with parasitic elements for mobile terminal. *IEEE Trans. Antennas Propag.* **60**(2), 473–481 (2012)
25. Y. Zhang, X.Y. Zhang, L.-H. Ye, Y.-M. Pan, Dual-band base station array using filtering antenna elements for mutual coupling suppression. *IEEE Trans. Antennas Propag.* **64**(8), 3423–3430 (2016)
26. A. Daggarpour, B. Zarghooni, B.S. Virdee, T.A. Denidni, A.A. Kishk, Mutual coupling reduction in dielectric resonator antennas using metasurface shield for 60 GHz MIMO systems. *IEEE Antennas Wirel. Propag. Lett.* **16**, 477–480 (2017)

27. D.H. Werner, S. Ganguly, An overview of fractal antenna engineering research. *IEEE Antennas Propag. Mag.* **45**(1), 38–57 (2003)
28. E. Guariglia, Entropy and fractal antennas. *Entropy* **18**(3), 84 (2016)
29. E. Guariglia, Harmonic Sierpinski gasket and applications. *Entropy* **20**(9), 714 (2018)
30. E. Guariglia, R.C. Guido, Chebyshev wavelet analysis. *J. Funct. Spaces* **2022**(1), 5542054 (2022)
31. H. Xu, H. Zhou, S. Gao, H. Wang, Y. Cheng, Multi-mode decoupling technique with independent tuning characteristic for mobile terminals. *IEEE Trans. Antennas Propag.* **65**(12), 6739–6751 (2017)
32. Y. Zhu, Y. Chen, S. Yang, Decoupling and low-profile design of dual-band dual-polarized base station antennas using frequency-selective surface. *IEEE Trans. Antennas Propag.* **67**(8), 5272–5281 (2019)
33. B. Yang, Y. Xu, J. Tong, Y. Zhang, Y. Feng, Tri-port antenna with shared radiator and self-decoupling characteristic for 5G smartphone application. *IEEE Trans. Antennas Propag.* **70**(6), 4836–4841 (2022)
34. Y. Zhang, S. Zhang, A side-loaded-metal decoupling method for $2 \times N$ patch antenna arrays. *IEEE Antennas Wirel. Propag. Lett.* **20**, 668–672 (2021)
35. Y. Li, Q. Chu, Dual-layer superstrate structure for decoupling of dual-polarized antenna arrays. *IEEE Antennas Wirel. Propag. Lett.* **21**, 521–525 (2022)
36. C.A. Balanis, *Antenna theory-analysis and design*, 3rd edn. (John Wiley & Sons, 2005)
37. Z. Xia and K.W. Leung, Gain enhancement of rectangular dielectric resonator antenna using EBG surface, *IEEE Asia-Pacific Conference on Antennas and Propagation (APCAP)*, Aug 2018
38. H.F. Shaban, H.A. Elmikaty, A.A. Shaalan, Study the effect of electromagnetic band-gap (EBG) substrate on two patches microstrip antenna. *Prog. Electromag. Res. B* **10**, 55–74 (2008)
39. M.K. Khandelwal, B.K. Kanaujia, S. Kumar, Defected ground structure: fundamentals, analysis, and applications in modern wireless trends. *Int. J. Antennas Propag.*, 2017

Publisher's Note

Springer Nature remains neutral with regard to jurisdictional claims in published maps and institutional affiliations.

Submit your manuscript to a SpringerOpen[®] journal and benefit from:

- Convenient online submission
- Rigorous peer review
- Open access: articles freely available online
- High visibility within the field
- Retaining the copyright to your article

Submit your next manuscript at ► [springeropen.com](https://www.springeropen.com)